Current Applied Science and Technology Vol. 22 No. 1 (January-February 2022)

Research article

Electrical Properties of Semiconducting Copper Zinc Sulphide Thin Films

Joseph Onyeka Emegha[1]*, Bolutife Olofinjana[2], Kingsley Eghonghon Ukhurebor[3], Joseph Taye Adegbite[4] and Marcus Adebola Eleruja[2]

[1]*Department of Physics, Faculty of Physical Sciences, University of Benin, Edo State, Nigeria*
[2]*Department of Physics and Engineering Physics, Obafemi Awolowo University, Ile-Ife, Nigeria*
[3]*Department of Physics, Faculty of Science, Edo State University Uzairue, Edo State, Nigeria*
[4]*Department of Geosciences, University of Lagos, Lagos, Nigeria*

Received: 24 October 2020, Revised: 17 February 2021, Accepted: 18 May 2021

DOI: 10.55003/cast.2022.01.22.003

Abstract

The electrical properties of metal-organic-chemical-vapour-deposited copper zinc sulphide (Cu-Zn-S) thin films on soda-lime substrates were studied. The films produced were characterized in terms of their electrical properties employing the Four-point probe procedure at a temperature range of 370 to 470°C. The electrical properties (resistivity and conductivity) of the deposited copper zinc sulphide films were systematically studied in terms of the deposition parameters of concentration and deposition temperature. The conductivity was in the interval of 5.48 to 8.0 × 10^{-1} $(\Omega.cm)^{-1}$. Activation energies of 0.54 and 0.29 eV in the deposition temperature range were estimated. The high resistive property of the films re-emphasized the potential use of these materials as active semiconductors for optoelectronic device applications.

Keywords

copper zinc sulphide;

electrical conductivity;

thin films;

thickness;

four-point probes

1. Introduction

Copper zinc sulphide (Cu-Zn-S) thin films are among the most important semiconducting materials in optoelectronic and spintronics device applications. They are direct wide band gap semiconductor

*Corresponding author: Tel.: +234(0)8068930891
E-mail: jjjemegha@yahoo.com

(1.6 - 3.50 eV) in the near and infrared regions [1, 2]. Copper zinc sulphide thin films have many advantages; high mechanical and chemical stability, flexible band gaps, non-toxic in nature, and high carrier mobility as well as useful abnormal luminescence properties [3, 4]. Due to their excellent opto-electrical properties, copper zinc sulphide thin films are potential materials for window layers in solar cell fabrication, flat-display panels, transparent conductors, organic light emitting diodes (OLEDs), mobile touch screens, gas sensors and so on [5, 6].

As reported by Emegha *et al*. [7], there are several reports of the diverse physical and chemical procedures that have been employed for the preparation of Cu-Zn-S thin films, such as "electron beam evaporation, electrochemical atomic layer deposition, solution growth techniques, chemical bath deposition, SILAR, chemical spray pyrolysis and metal-organic chemical vapour deposition (MOCVD) technique". Among these methods, the MOCVD technique is of the highest interest because of the advantages gained by using several "single solid source precursors". A single solid source precursor provides a novel approach with the advantages of minimizing the shortcomings of the conventional methods due to the use of two or more precursors with different chemical properties. This technique has been found to be more efficient in the preparation of clean and uniform films as the stoichiometry and deposition temperature are controlled by the design variables [8].

In our previous papers [4, 7], copper zinc sulphide thin films were prepared on soda-lime substrates using mixed copper and zinc dithiocarbamate precursors. X-ray diffraction (XRD) study revealed polycrystalline films with no secondary phase formations. Surface morphology of the films were observed with scanning electron microscopy (SEM), and indicated that the Cu-Zn-S films consisted of well-defined grains with dense interconnections that were free from cracks and pinholes. The elemental analysis showed a material consisting of copper, zinc and sulphur in various stoichiometric ratios. Besides the elemental studies, Rutherford backscattering (RBS) was also used to determine the thicknesses of the films using knowledge of the material density. The analysis of the optical transitions indicated that the deposited films had a direct optical bang gap that varied from 2.20 to 3.42 eV with increase in zinc concentrations. The thickness, refractive index, transmittance, extinction coefficient and optical conductivity were found to depend on the deposition parameters. In the present research, our previous study has been completed by providing the electrical results obtained from the mixed copper and zinc precursors. The influence of copper/zinc concentrations as well as the deposition temperature on the electrical conductivity of metal-organic chemical vapour deposited copper zinc sulphide thin films was investigated. The activation energy was also estimated and discussed within a deposition temperature range of 370 to 470^{o}C.

2. Materials and Methods

2.1 Growth of the films

Cu-Zn-S thin films were grown on clean substrates (soda-lime) via the MOCVD method. Copper dithiocarbamate and zinc dithiocarbamate were used as starting materials in the fabrication process. Variations of the copper and zinc concentrations in Cu-Zn-S thin films were achieved by depositing the precursors at a constant deposition temperature of 400^{o}C for 2 h at a flow rate of 2.0 dm^3/min. Details of the deposition process as reported in the past work [7], are shown in Table 1.

The thickness was estimated using the Rutherford Backscattering Spectroscopy (RBS) technique and ranged between 25.9 and 57.6 nm (Table 1) [7], while the "Four-point probe" was employed for evaluating the electrical properties of the films. Four samples of $Cu_xZn_{1-x}S$ films with

several concentrations (× = 0.9, 0.7, 0.3 and 0.1) were formed and categorized as A1, A2, A3 and A4, and are shown in Table 1.

Table 1. The concentration percentage (%) of the film samples and their thickness

Samples	Molecular Precursors	Thickness (nm)
A1	90% copper dithiocarbamate + 10% zinc dithiocarbamate	44.5
A2	70% copper dithiocarbamate + 30% zinc dithiocarbamate	57.6
A3	30% copper dithiocarbamate + 70% zinc dithiocarbamate	52.3
A4	10% copper dithiocarbamate + 90% zinc dithiocarbamate	25.9

2.2 Theoretical consideration

The four-point probe, also known as four-wire sensing, is commonly used for semiconductor material characterization [9]. This probe is usually used to measure the sheet resistivity of thin conducting films. The electrical resistivity (ρ) describes the basic class of any electrical substance as a conductor, insulator or semiconductor. Consequently, ρ constitutes one of the main basic properties that should be quantified or measured during the exploration of new substances for electronic applications [10]. One of the simplest and utmost techniques for measuring the ρ in a thin film is by applying a two point-probe arrangement, where each contact functions as a current (I) and as a voltage (V) probe source. However, this arrangement has some limitations, which result from the measured resistance being critically affected by the resistance (R) which is being probed and the contact R between each metal probe and the semiconducting material [11]. Hence, it is often preferred to apply a "four-point probe arrangement", where I is applied between the two points and V is measured with two extra contacts.

There are different four-point probe configurations that can be used, and the most common ones are:

a) The collinear configuration, where four similarly set apart probes are positioned on top of the film. The two outer probes are employed for spacing I while the subsequent V is measured via the two inner probes.

b) The Van der Pauw configuration, which usually consists of four minor electrodes on the edge of a smooth, subjectively shaped sample of unvarying thickness.

The first configuration was employed to investigate the films formed during this study, and it was done via Old Jandel four-point probe technique (Model TY242MP). The arrangement was carried out in a manner that the V across the diagonal distance of the films and the equivalent values of the I were measured by means of a silver paste in order to guarantee a good Ohmic contact to the film. The values of R for the films were investigated. The four-point probe was linked to a current supply and the inner probes to a volt meter. As shown in Figure 1, I was applied between outer probes and the resulting V was measured by the two inner probes.

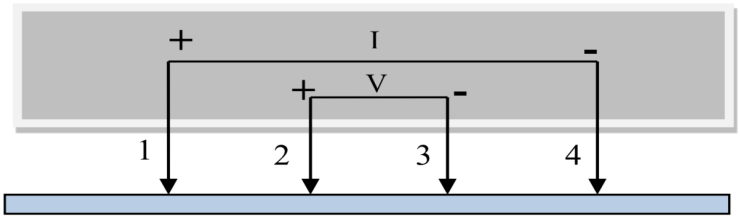

Figure1. Four-point probe configuration [12]

The principle of the (four-point probe) configuration applied for this study was based on Ohm's law. In this case, the *R* is expressed by the resistivity and the geometry of the films [13].

$$\Delta R = \rho\left(\frac{dx}{A}\right) \tag{1}$$

For bulk substances where thickness (t) is far greater than the probe distance (s), *I* penetrates spherically into the films; thus, the affected area is $A = 2\pi X^2$ [12]. From equation (1), the integration between the inner probe's tips, that is where the *V* is measured, gives:

$$R = \frac{1}{2s}\frac{\rho}{2\pi} \tag{2a}$$

S is the probe spacing and the superposition of *I* at the outer two tips is;

$$R = \frac{V}{2I} \tag{2b}$$

Therefore, modifying the equation for bulk resistivity in (2a) gives:

$$\rho = 2\pi S\left(\frac{V}{I}\right) \tag{3}$$

If the films are very thin (thickness t <<s), *I* ring is attained as an alternative of sphere. Substituting $A = 2\pi xt$ into the resistance equation (1), it becomes:

$$R = \int_s^{2s} \rho\frac{\rho}{2\pi x^2} = \frac{dx}{x} - \frac{\rho}{2\pi t}\ln(x)\Big|_s^{2s} \tag{4}$$

$$R = \frac{\rho}{2\pi t} ln\, 2 \tag{5}$$

Hence, for $R = \frac{V}{2I}$, $\rho$for a thin sheet is:

$$\rho = \frac{\pi t}{\ln 2}\left(\frac{V}{I}\right) = 4.532t\left(\frac{V}{I}\right) \tag{6}$$

Sheet resistance (R_s) is the ρ without taking into account the thickness of the films [12]. R_s was evaluated by taking the slope of *V* to *I* relation obtained via the four-point probe data. Therefore;

$$R_S = 4.532\left(\frac{V}{I}\right) \quad (7)$$

and

$$\rho = \mathrm{R_s} \times \mathrm{t} \quad (8)$$

The electrical conductivity (σ)was taken as the reciprocal of the electrical resistivity given in equation (9)

$$\sigma = \frac{1}{\rho} \quad (9)$$

Electrical conductivity of Cu-Zn-S thin films generally depends on the deposition temperature. Hence, the connection between the deposition temperature and the activated conductivity of the deposited films follows the Arrhenius law and is given by equation (10):

$$\sigma = \sigma_o \exp\left(-\frac{\Delta E}{2kT}\right) \quad (10)$$

σ is the electrical conductivity, σ_o is the conductivity at absolute temperature, T is the absolute temperature, k is the Boltzmann constant, and ΔE is the activation energy of the electrical conductor [14]. Depending on the conduction mechanism of the semiconductor, the Arrhenius equation can be extended to equation (11):

$$\sigma = \sigma_1 \exp\left(-\frac{\Delta E_1}{2kT}\right) + \sigma_2 \exp\left(-\frac{\Delta E_2}{2kT}\right) \quad (11)$$

where ΔE_1 and ΔE_2 are the activation energies corresponding to the two conduction regions.

3. Results and Discussion

Figure 2 shows the average voltage and the corresponding current of sample A1. The other samples show similar linear plots. The electrical conductivity σ, resistivity ρ and sheet resistance R_s, of the deposited films are presented in Table 2. From Figure 2, the graph was found to be smooth and non-ohmic which clearly indicates that the deposited Cu-Zn-S films are semiconducting in nature. It was also observed that the current flowing through the films increased with the voltage of the electrodes. The observed increased in forward current at all voltages obtained for the films indicates the higher conductivity of these films. This improved forward current could be helpful in obtaining increase efficiency in solar cell production [15].

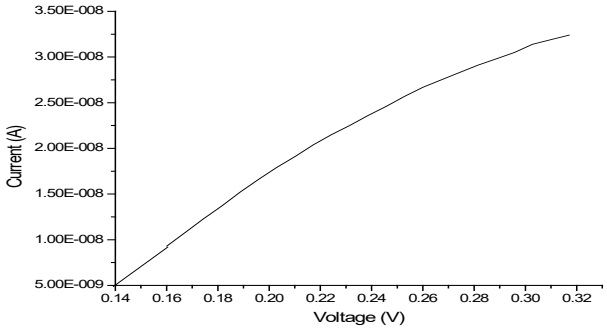

Figure 2. Current-voltage characteristic of sample A1

Table 2. Some electrical properties of Cu-Zn-S thin films

Samples	Sheet resistance (Ω/Sq.) × 10^7	Resistivity (Ω.cm) × 10^{-2}	Conductivity $(\Omega.cm)^{-1}$
A1	0.41	18.25	5.48
A2	2.26	130.09	0.77
A3	1.22	63.79	1.57
A4	15.20	392.92	0.26

The variation of the electrical resistivity and conductivity of the various samples are presented in Figure 3. From the Figure, the electrical resistivity was found to increase from sample A1 to A2, and then reduces to A3. As the concentration of copper decreases, the resistivity increased more rapidly to the highest value at A4. The electrical conductivity followed the opposite pattern as illustrated in Figure 3. The decrease in resistivity experienced within the samples was due to the production of more pairs of electrons and holes occasioned from zinc incorporation in the Cu-Zn-S system. Further increment in zinc concentrations (sample A4) led to a rise in resistivity due to phase transformation and associated distortions of the Cu-Zn-S thin films.

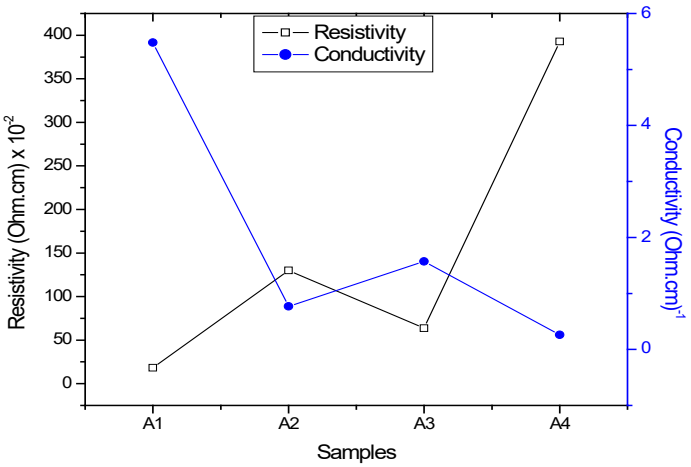

Figure 3. Variation of the resistivity and the conductivity with different samples

In addition, the average electrical conductivity falls and rises within the range of 10^{-3} to 10^2 reported for semiconducting thin films in the literature [16], which suggests that the electrical properties are a function of the intrinsic defects within the films. The defects thus introduce donor states in the forbidden bands just below the conduction band and therefore result in the conducting nature of the films.

To determine the total electrical conductivity of the Cu-Zn-S material, the deposition temperature of sample A2 ($Cu_{0.7}Zn_{0.3}S$) was extended to 370, 400, 430, 450 and 470°C. Sample A2 was chosen because the films have a relatively better adhesion to the substrate. From equation (10), the activation energy was determined by the slope of the linear part of the graph of ln(σ) against 1000/T (Figure 4). From the Figure, there are two straight lines that correspond to the two terms (ΔE_1 and ΔE_2) of equation (11). These terms indicate that there are two different conductivity

mechanisms of Cu-Zn-S thin films within the temperature range of 370 and 470°C. The slopes of these lines give the estimated activation energies of the regions. In the high temperature region (region 1), the conductivity increases relatively faster with deposition temperatures due to the extrinsic nature of the deposited material. This temperature region is given by the ΔE_1 in equation (11). The transition in this region depends on two variables; the deposition temperature and the lattice vibration [17]. As the deposition temperature is elevated, the charge carriers are increased, which leads to an increase in the material conductivity. However, the lattice vibration creates electron-photon interactions which cause hindering of electrons, so electrons need more energy to

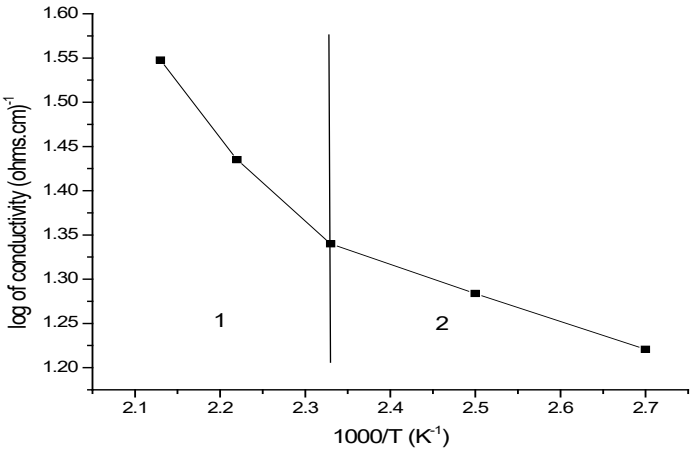

Figure 4. Variation of logarithmic conductivity with the inverse absolute temperature of Cu-Zn-S thin films

be activated. In the low temperature regions (region 2), the σ increases slowly with deposition temperature. According to Rahman *et al.* [18], this slow increment of σ could be linked to the hopping of carriers within the localized states.

In region 1, which are the regions with higher deposition temperature, the value of the estimated activation energy was given as ΔE_1=0.54 eV. While in the low deposition regions (region 2), the value was ΔE_2 = 0.29 eV. The values of the estimated activation energies of Cu-Zn-S thin films confirmed that the deposited material was a semiconductor [17]. It was also observed that in the higher deposition temperature region, the estimated value of the activation energy was higher than that in the lower region. Such trend indicates that charges moved from one conduction mechanism to another. The higher activation energy value in this region could be ascribed to the fact that the energy required to form the defects is far greater than that which is require for its drift [19].

4. Conclusions

In this study, the electrical properties of Cu-Zn-S thin films deposited by MOCVD were measured. The sheet resistance, electrical resistivity, conductivity and activation energies were studied and correlated with the samples and deposition temperatures of the films. It was observed that Cu-Zn-S thin films had two temperature regions that were connected to the conduction mechanism of the deposited material. The calculated values of the activation energies revealed that the deposited

materials were semiconductors. The obtained results confirmed that Cu-Zn-S thin films are useful materials for optoelectronic applications such as touch and gas sensors, transparent resistors, spintronics and piezoelectricity.

5. Acknowledgments

The authors are particularly grateful to the Department of Physics, Obafemi Awolowo University, Ile Ife, Nigeria for providing the facility used for this study.

References

[1] Jose, E. and Kumar, M.C.S., 2017. Room temperature deposition of highly crystalline Cu-Zn-S thin films for solar cell applications using SILAR method. *Journal of Alloys and Compound,* 712, 649-656.

[2] Kitagawa, N., Ito, S., Nguyen, D. and Nishino, H., 2013. Copper zinc sulfur compound solar cells fabrication by spray pyrolysis deposition for solar cells. *Natural Resources*, (4),142-145.

[3] Emegha, J.O., Damisa, J., Efe, F.O., Olofinjana, B., Eleruja, M.A. and Azi, S.O., 2019. Preparation and characterization of metal organic chemical vapour deposited copper zinc sulphide thin films using single solid source precursors. *European Journal of Materials Science and Engineering*, 4(1), 11-22.

[4] Emegha, J.O., Okafor, C.M. and Ukhurebor, K.E., 2021. Optical properties of copper-zinc sulphide network from mixed single solid source precursors of copper and zinc dithiocarbamates. *Walailak Journal of Science & Technology*, 18(9), https://doi.org/10.48048/wjst.2021.9535.

[5] Alkhayatt, A.H.O., Habieb, A.A.W., Al-Noaman, A.H.A. and Hameed, A.A., 2019. Structure, surface morphology optical properties of $Cu_xZn_{1-x}S$/Au NPs layer for photo detector application. *Journal of Physics: Conference Series*, 1234, 012012, https://doi.org/10.1088/1742-6596/1234/1/012012.

[6] Jubimol, J., Sreejith, M.S., Kartha, C.S., Vijayakumar, K.P. and Louis, G., 2018. Analysis of spray pyrolysed Copper zinc sulfide thin film suing photoluminescence, *Journal of Luminescence*, 203, 436-440.

[7] Emegha, J.O., Olofinjana, B., Eleruja, M.A., Efe, O. and Azi, S.O., 2019. Preparation and physical properties of $Cu_xZn_{1-x}S$ thin films deposited by metal organic chemical vapour deposition technique. *Journal of Materials Science Research and Review,* 2(4), 1-9.

[8] Ilori, O.O., Osasona, O., Eleruja, M.A., Egharevba, G.O., Adegboyega, G., Chiodelli Boudreault, G., Heynes, C. and Ajayi, E.O.B., 2015. Preparation and characterization of metalorganic chemical vapour deposited $Li_xMo_yO_z$ using a single source solid precursor. *Ionic*, 11, 387-391.

[9] Chandra, N., Sharwa, V. and Chung, G.Y., 2011. Schroder. Four-point probe characterization of 4H Silicon carbide. *Solid-State Electronics*, 64, 73-77.

[10] Barquinha, P.M.C., 2010. *Transparent Oxide Thin-film Transistors; Production, Characterization and Integration*. Ph.D. Universidade Nova De Lisboa, Portugal.

[11] Schroder, D.K., 2006. *Semiconductor Material and Device Characterization*. 3rd ed. New Jersey: John Wiley & Sons.

[12] Herodotou, S., 2015. *Zirconium Doped Zinc Oxide Thin Films Deposited by Atomic Layer Deposition.* Ph.D. The University of Liverpool, United Kingdom.

[13] Yu-Hsiu, L., 2009. *Structure and Properties of Transparent Conductive ZnO Films Grown by Pulsed Laser Deposition (PLD)*. M.Sc. University of Birmingham, United Kingdom.
[14] Patidar, D., Rathore, K.S., Saxena, N.S., Sharma, K. and Sharma, T.P., 2008. Energy band gap and conductivity measurement of CdSe thin films. *Chalcogenide Letters*, 5(2), 21-25.
[15] Thirumavalavan, S., Mani, K. and Sagadevan, S., 2015. Investigation of the structural, optical and electrical properties of copper selenide thin films. *Materials Research*, 18(5), 1000-1007.
[16] Emegha, J.O., Elete, D.E., Efe, F.O. and Adebisi, A.C., 2019. Optical and electrical properties of semiconducting ZnS thin film prepared by chemical bath deposition technique. *Journal of Materials Science Research and Reviews*, 4(1), 1-8.
[17] Hassanien, A.S. and Akl, A.A., 2016. Effect of Se addition on optical and electrical properties of chalcogenides CdSSe thin films. *Superlattices and Microstructures*, 89, 153-169.
[18] Rahman, M.M., Khan, M.K.R., Islam, M.R., Halim, M.A., Shahjahan, M., Hakim, M.A., Saha, D.K. and Khan, J.U., 2012. Effect of Al doping on structural, electrical, optical and photoluminescence properties of nano-structural ZnO thin films. *Journal of Materials Science andTechnology,*28(4), 329-335.
[19] Colak, H., 2015. Influence of Tm_2O_3 doping on structural and electrical properties of ZnO. *Journal of Materials Science, Materials. Electronics*, 26(2), 784-790.